

A Holistic Routing Protocol Design in Underground Wireless Sensor Networks

Di Wu, Renfa Li

School of Computer and Communication
Hunan University, Changsha, China

Lichun Bao

Donald Bren School of ICS
University of California, Irvine, USA

Abstract

The traditional networking builds on layered protocol architecture to isolate the complexities in different layers. It has been realized that real-life wireless sensor networks (WSNs) must be considered holistically across different layers for optimum performance. We consider a special case of WSNs that is deployed in underground tunnels. Underground communications present unique signal propagation characteristics due to the geographic and geological features, which in turn impact the underground network deployment and multi-hop routing patterns. We propose an efficient routing algorithm, called BRIT (Bounce Routing in Tunnels), for underground WSNs, and evaluate BRIT against the bottomline AODV in terms of network throughput, packet loss rate, stability and latencies using simulations. The contributions of the paper include a hybrid signal propagation model in three dimensional underground tunnels, an assortment of sensor deployment strategies in tunnels, an integrated routing metric (forwarding speed), and a route suppression mechanism.

1 Introduction

Wireless sensor networks (WSNs) are becoming a critical part of the information infrastructure in industrial control, environmental monitoring and human life rescue operations, and have been widely studied and deployed in real life operations. Especially in light of coal mine disasters in recent years, governmental supports in this area have given unprecedented attentions to the research, development and deployments of WSNs to serve data communication purposes in mining tunnels.

In WSNs, beside the critical research problems such as energy consumptions and network capacity planning, network routing efficiency stands out as the pivotal factor [14]. We study the cross-layer design issues for routing in WSNs that are deployed in underground mines and tunnels.

In mining environments, the unique challenges come from the geographic shapes and textures of the tunnels, which in turn affect various aspects of data communication features in terms of signal propagation, deployment and networking techniques [6], [20]. The modeling of these characteristics and the designing networking protocols become so intertwined that it requires a cross-layer perspective in underground mining environments.

Emslie *et al.* studied the radio communication properties in coal mines, and discovered the radio frequency ranges that allow RF signals traverse tunnels with the least loss [6]. Nerguzian *et al.* further explored and presented results about the 2.4Ghz ISM band radio propagation characteristics in underground mines [15].

Recently, an emerging communication technology that uses Impulse Radio Ultra Wide Band (IR-UWB) has been extensively studied [4], [21]. IR-UWB can potentially provide high data rate, highly accurate ranging, and strong resistance to multi-path and interference, thus becomes the ideal choice of underground communication in tunnels. Li *et al.* explored the applicability of UWB channels in coal mines for underground communication purposes [11] and Sheng *et al.* discussed the feasibility of modeling propagation model based on the free-space model for UWB systems [7].

Many networking algorithms have been proposed according to the unique characteristics of underground tunnels. Kim *et al.* analyzed the spatial reuse through tuning transmit power, carrier sense threshold and data rate [9]. Li *et al.* proposed the structure-aware self-adaptive WSN [13], and later designed a render-path way for hole management and routing based on location [12]. Furthermore, the geographic information [10], [2] and virtual coordinate [19] were applied for routing and boundary recognition purposes, respectively.

However, because of the complexities of underground tunnel communication systems, a holistic design paradigm has to be considered, and a cross-layer design of routing protocols are necessary for efficient communication in underground tunnel environments. Tunnel modeling in three dimensions [1], signal propagation models [3], [5], sensor deployment patterns are the key factors to be considered in order to provide a practical routing protocol in such environments.

Our contributions in this paper are many folds. After first characterizing and modeling the mining tunnel environments in terms of the tunnel geometry, we present

This work was sponsored in parts by the Raytheon Company under Grant No. RC-42621, the National Natural Science Foundation of China under Grant No. 60673061, the National Research Foundation for the Doctoral Program of Higher Education of China under Grant No. 20060532024, and the National Key Project of Scientific and Technological Support under Grant No. 2007BAK23B03.

- A novel hybrid signal propagation model that combines the traditional free-space and two-ray ground propagation models according to the 3D modeling of tunnels.
- A study of popular wireless sensor network deployment strategies, namely the random, bipartite, spiral and lineup deployments.
- A new on-demand routing algorithm, named BRIT (Bounce Routing in Tunnels), which takes advantage of the mining environments. The name “bounce” came from our routing heuristic that mimics the passing of a ball through a tube. Similar to the analogous ball that has to bounce on the inner surface multiple times in order to traverse from one end of the tube to the other, wireless packets have to pass through the mining tunnels in multiple steps.
- A novel routing metric, called “forwarding speed”. In our bounce-ball heuristics, to achieve fastest speed of passage through the tunnel, the trajectory of the ball intersects with the tube surface with minimum angle at each hop and with least loss of energy. Therefore, the “forwarding speed” tries to provide a similar and single metric for optimal selection of intermediate hops in ad hoc networks based on information such as the transmission rates in multi-rate wireless networks, each forwarding node’s queuing status and adjacent nodes’ distance information.
- A route suppression mechanism that avoids flooding effects of route discovery messages.

The rest of the paper is organized as follows. Section 2 presents the assumptions about the underground mining environments and about WSNs, then we discuss several sensor network deployment strategies. Section 3 describes and formulates the propagation models in tunnels. Section 4 specifies the BRIT routing algorithm in details. Section 5 evaluates our mining environment models as well as our routing algorithm using simulations. The performance of our routing algorithm is compared with other signal propagation models and routing protocols in similar settings. Section 6 summarizes the paper and its key contributions.

2 Deployment Strategies

2.1 Network Assumptions

In this paper, we assume that sensors are calibrated with their respective location information in the tunnels ahead of time so that they may fully utilize the location information and derive relative positions between nodes in the three-dimensional space. Such assumption is not an overly extraneous burden because wireless sensor networks are relatively static attached in tunnels, and many localization algorithms could be applied to derive such information. Especially in underground mining tunnels, location information is important in localizing miners and assessing damages in search and rescue operations. We propose deployment strategies, propagation modeling and the BRIT routing algorithm based on the accurate knowledge of sensor locations.

2.2 Mine Geographic Model

Our mine geographic model is based on the measurements of Chatang coal mine, which was part of an ongoing collaborative project with the Baisha Coal Corporation in Chenzhou, China. The mining area is 1.8225 km^2 with four mine fields. The main tunnel starts from the ground surface, and extends along a sloped angle for 6783 m into the 128.4 m deep underground working bed. The tunnel cross-section is approximately 4 m wide and 3.5 m high.



Fig. 1. Photograph of The Coal Mine Tunnel.

Fig. 1 shows a part of the main tunnel supported by the metal framework. The walls are rough, and the floor is rugged, covered with coal cinders and waste materials.

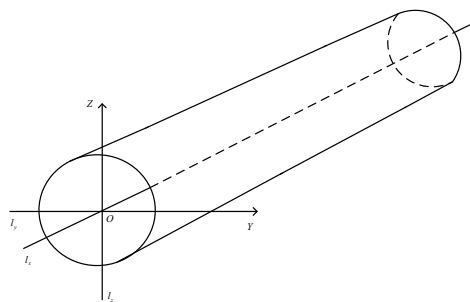


Fig. 2. Cylindrical Model of the Coal Mine Tunnel.

For simplicity and without loss of generality, we model the coal mine tunnels and other similar structures as smooth cylindrical hollow tubes with three dimensional coordinate as shown in Fig. 2.

2.3 Sensor Node Deployment Strategies

Several deployment strategies have been commonly considered in practice to place sensor nodes along the cylindrical tunnels. We enumerate and explain some of these strategies in this section, and present evaluation results regarding each of them later with regard to the impact on the network performance. Note that we have assumed location information is calibrated and stored on the sensors in any of these deployments. For convenience, we denote that N_s sensor nodes will be deployed along the surface of the cylindrical tunnels.

Random Deployment: In this strategy, the nodes are randomly attached to the inner surface of the cylindrical tunnel using a uniform distribution function. It was a common belief that randomness provides network robustness, which we will evaluate later.

Line-up Deployment: In this strategy, the nodes are evenly placed along a single straight line on the ceiling of the tunnel.

Bipartite: The sensor nodes are divided into two equal groups, and the sensors of each group are attached to one side of the cylindrical tunnel, separately, each along a straight line parallel to the tunnel axis.

Spiral Deployment: The nodes are deployed in equal distance to each other along a spiral curve winding down the tunnel surface. The distance between successively deployed sensors depends on the length the spiral line through the tunnel, which in turn depends on the starting angle of the spiral curve with regard to the tunnel axis.

3 Tunnel Propagation Model

Radio signal propagates and behaves very differently in underground tunnels from the textbook flat-surface assumptions. We first review the two common-used signal propagation models, then adapt these models in an underground tunnel settings to study the signal propagation characteristics in UWB-based sensor networks.

3.1 Free-Space Propagation Model

In the free-space propagation model, we assume that the RF transmitter and receiver have an unobstructed line-of-sight path between them. Accordingly, we know that received power decays by the square power of the transmitter-receiver distance d , as shown by the Friis free-space signal propagation equation [18]:

$$P_{fs}(d) = P_t G_t G_r \frac{\lambda^2}{(4\pi)^2 d^2 L}, \quad (1)$$

where $P_{fs}(d)$ is the received signal power which is a function of the transmitter-receiver distance d . P_t is the transmission power, G_t and G_r are the transmit and receive antenna gains, respectively. L is the system loss factor, which is set to $L \geq 1$ usually, and λ is the RF wavelength in meters.

3.2 Two-Ray Model

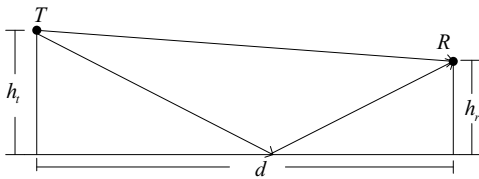


Fig. 3. Two-Ray Signal Propagation Model.

The two-ray signal propagation model comes from the fact that RF signal beams achieve near-complete reflection of their

energy when the signal beams arrive at the boundary of two media and the incidental angle of the signal rays in the transmission medium is below certain threshold. Under such conditions, the straight light-of-sight rays and the reflected rays become phase-canceling interference to each other at the receiver, and the signal power drops at the rate of power four in the two-ray model instead of power two in the free-space model. Fig. 3 illustrates such effects, and Eq. (2) provides the relationship between the received power and other factors [18].

$$P_{tr}(d) = P_t G_t G_r \frac{h_t^2 h_r^2}{d^4} \quad (2)$$

where $P_{tr}(d)$ is the received signal power which is a function of the transmitter-receiver distance d , h_t and h_r are the heights of the transmit and receive antennas, respectively, and the two-ray model is effective when $d \gg \sqrt{h_t h_r}$. Other factors have similar meanings as in Eq. (1).

3.3 Tunnel Propagation Model

Signal propagations in underground tunnels are a special case of those along the flat surfaces, and have very different results from the aforementioned two models.

There are mainly two types of RF signal propagation scenarios in underground tunnels — one is near the tunnel surface, and the other within the tunnel hollow space. Fortunately, these patterns can be approximated by the two-ray and free-space models, respectively. Therefore, for practical evaluations of communication systems in tunnel environments, we propose and describe a hybrid model that combines the free-space and two-ray propagation models adaptively under the cylindrical geometric model.

Free-Space Propagation Model: In free-space propagation model, an important concept was *Fresnel zone*. Fresnel zones look like concentric onion layers in a 3D illustrations, and are numbered from one upwards starting from the inner most layer. The first Fresnel zone carries the strongest signal from the transmitter to the receiver. If any obstacle exists in the layers, then the obstacle in odd numbered zones diffracts and creates constructive signals at the receiver, and that in even numbered zones provides destructive signals at the receiver.

Because we have adopted a smooth cylindrical hollow tube-like surface for underground tunnels, the only obstacle in our tunnel model is the tunnel walls. Therefore, the primary Fresnel zone, *i.e.* the first Fresnel zone, is only limited by the width and height of the tunnel. We apply the Fresnel theory to calculate the farthest distance that the free-space model can reach, which is given by Eq. (3) [11].

$$d_{NF} = \frac{R^2}{\lambda}, \quad (3)$$

where R is the diameter of the idealized tunnel model in this paper.

Hence, according to the Fresnel theory, signal power attenuates in the free-space model using Eq. (1) when the transmitter-receiver distance is less than d_{DF} given by Eq. (3).

In our research project at the Chatang coal mine, the tunnel is about four meters in diameter. If we use UWB communication system with center frequency 5GHz, d_{NF} in the

propagation area of main tunnel is about 200m. Therefore, it is safe to apply the free-space model to describe the propagation of UWB signals in hollow space.

Two-Ray propagation model: When sensors are placed in tunnels, the effective antenna heights in the two-ray model are greater than the actual heights because of the cylindrical tunnel surface curvature.

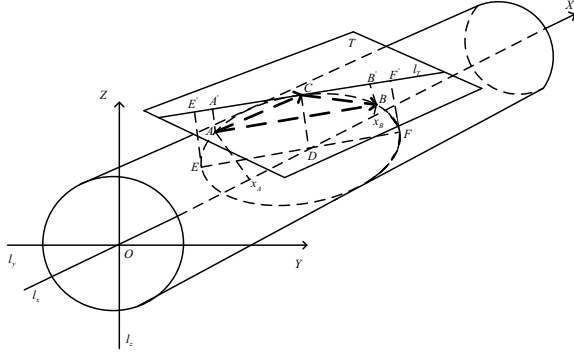


Fig. 4. Effective Antenna Height in the 3D Model.

Fig. 4 illustrates the formation of two-ray model in tunnels, where point A is the transmitter, point B is the receiver, point C is the reflection point, and plane T is the tangent plane of the tunnel at point C .

Without detailed proof, we conjecture that there are only two reflection points in a cylindrical tunnel between any two points — one on each side of the line between the transmitter and the receiver. Because of the small incident angle requirement in the two-ray model, we only consider one of the reflected signals.

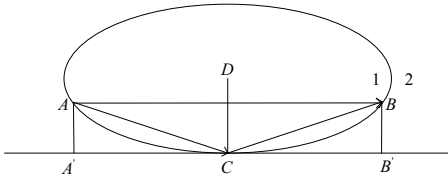


Fig. 5. Cross Section of The Two-Ray Propagation Model in Tunnels.

Fig. 5 illustrates the effective heights of antennas of two sensor nodes in the cross section of the cylindrical tunnel model. Unlike the flat-surface assumption in the textbook two-ray model, the antenna heights h_t and h_r in Eq. (2) changes according to the locations of the transmitter and the receiver. When points A and B are closeby, their antenna heights are almost zero. When they separate with each other, their antenna heights gradually increase. In the course of the antenna changes, the propagation model would change between free-space and two-ray models.

Hence, the critical factor is the effective antenna heights h_t and h_r of Eq. (2) in determining whether the free-space model or the two-ray space model is applied. In order to derive h_t and h_r , we calculate the coordinates of the reflection point C

in Fig. 4. Because of the symmetric nature of points A and B in the cylindrical tunnel, it is easy to prove that point C is at the mid-point between nodes A and B , and that $h_t \equiv h_r$. Accordingly, we can easily calculate the coordinates of point C in Fig. 4, then derive heights h_t and h_r with the help of points A , B , C and D in Fig. 5.

Combining Free-Space and Two-Ray Models: We use a combination of free-space and two-ray propagation models to represents the signal preparations model in our cylindrical tunnel model.

As we mentioned, free-space propagation model could be applied in mine tunnel for hundreds of meters when the frequency of radio signal's pulse is in the order of GHz. However, Eq. (1) is mainly used for narrowband signal. Because the power spectral density (PSD) of UWB signal's pulse is very wide, we need to modify Eq. (1) to account for variations across the bandwidth of the signal. If we assume that the received signal occupies a band from f_L to f_H , we have following relation about the transmit range of UWB signal in free-space propagation model [7]:

$$d = \frac{c}{4\pi} \sqrt{\frac{A_{max} G_t G_r}{E_b/N_0 \cdot R_b \cdot k T_0 F \cdot LM} \int_{f_L}^{f_H} \frac{|P_n(f)|}{f^2} df}, \quad (4)$$

where $A_{max} = -41$ dBm/MHz is the maximum PSD permitted by FCC, $|P_n(f)|$ is the normalized PSD, R_b is the bit rate, E_b/N_0 is the bit energy and N_0 is the noise spectral density. E_b/N_0 is the bit signal-to-noise ratio, $N_0 = k T_0 F \cdot LM$, where k is Boltzmann's constant 1.38×10^{-23} Joules/K, T_0 is normal temperature, F is the noise figure, LM is the link margin.

For our UWB systems in mine tunnel, we have normal mine temperature $T_0 = 300$ K, $F = 6$ dB and $LM = 5$ dB. So the noise spectral density N_0 in mine tunnel approximates -102.83 dBm/MHz. For one-order derivatives of the Gaussian UWB pulse with f_M 4.79 GHz, f_H could be 7.84 GHz and f_L could be 2.31 GHz. Furthermore, we get the additional loss caused by coal carrier is 10-13dB, caused by slicers is 5-10dB, caused by hydraulic pressure pump is 5-8dB, caused by transmitting strap is 5.8dB.

On the basis of above wideband free-space model and system parameters, we provide a reliable strategy to combine free-space and two-ray propagation model for signal estimation in underground tunnel. The boundary condition to switch between the two basic propagation models is $P_{fs} \equiv P_{tr}$, and we determine the received signal power using Eq. (5).

$$P_r = \min(P_{fs}, P_{tr}), \quad (5)$$

where P_{fs} and P_{tr} were given in Eq. (1) and Eq. (2).

Equivalently, we can determine the choice of free-space and two-ray propagation models by calculating

$$\frac{P_{fs}}{P_{tr}} = \frac{(4\pi)^2 L h_t^2 h_r^2}{\lambda^2 d^2} \quad (6)$$

Suppose that the cylindrical tunnel is 4m wide and 100m long, that the transmit power is 1.4×10^{-4} Watts and the receive threshold of the received power is 1.4×10^{-11} Watts, and that a transmitter is located at the mid-surface of the

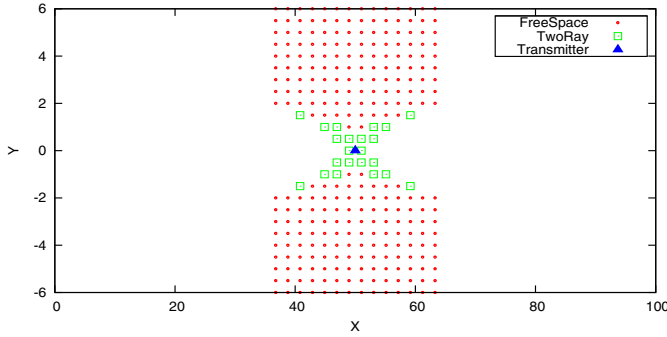


Fig. 6. The Application of Free-Space and Two-Ray Models in Tunnels.

tunnel, Fig. 6 illustrates the square points that may receive signals from the transmitter through the two-ray model, and circular points that may receive signals through the free-space model. Other points at the blank space are not able to receive signals.

4 BRIT Routing Protocol Specification

In our BRIT routing algorithm, we exploit and integrate physical propagation models, tunnel geographic models and location information as much as possible to provide the near optimal routing paths to guarantee the quality of service (QoS) for our multimedia applications.

BRIT is an on-demand routing protocol that follows the same route discovery and route maintenance scheme as adopted by AODV [16] and DSR [8]. However, due to the unique geographic nature of underground tunnels, it is usually unnecessary to implement flooding to explore possible paths during the route discovery phase to reach certain destinations, or maintain multiple paths for robustness purposes. Especially, in wireless sensor networks, many of the robustness provisioning in mobile environments can be simplified and eliminated.

In the following sections, we address issues regarding location-based route discovery and routing message suppression for data forwarding in underground tunnel environments. In specific, we introduce a new forwarding metric, called *forwarding speed*, that is applicable in location-based routing schemes.

Note that the following discussions, we focus on a single RREQ message to discuss ways to improve routing performance.

4.1 Location Awareness Route Discovery

In BRIT, a route is established when the source node sends a RREQ (route request) message in search of a path to certain destination, and receives a RREP (route reply) message in return. For this purpose, AODV is adapted to implement BRIT.

Fig. 7 illustrates the generic behaviors of RREQ message forwarding in the original AODV specifications.

Forwarding Speed: In order to find the path from any sensor source to the sink destination, we define a new metric, called

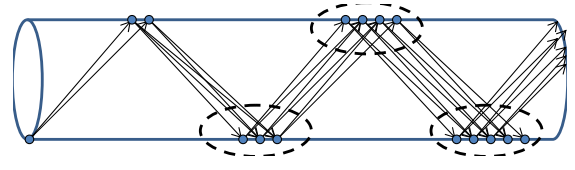


Fig. 7. RREQ Message Forwarding Scenario in the Original AODV.

forwarding speed, for an RREQ receiver to evaluate the quality of the potential path through itself. The forwarding speed $S_{forward}$ is a vector, defined by Eq. (7).

$$S_{forward} = \frac{D_{RREQ}}{T_{Queue} + T_{MAC}}, \quad (7)$$

Eq. 7 deserves a careful explanation with regard to each terms:

- D_{RREQ} is the vector between the current RREQ transmitter to the receiver projected onto the vector between the source and destination of the RREQ message. The value of D_{RREQ} is easily computable because of our assumption on location information. The positive direction of the forwarding speed vector points to the destination location.
- T_{MAC} is the average medium access delay to transmit a packet at the RREQ receiver. T_{MAC} is approximated by the channel access control overhead (*i.e.* the sum of RTS/CTS/ACK transmission times and deferral/backoff latencies) plus the data packet transmission time. Note that data packet transmission time is not the RREQ message transmission time because the RREQ messages are broadcast, and the broadcast data rate is usually not optimized for unicast data forwarding purposes in multi-rate communication networks. Therefore, when we evaluate the quality of a path using Eq. (7), we need to derive the unicast forwarding speed using the SNR (signal-to-noise ratio) or the RSSI (received signal strength indicator) information of the received RREQ messages. According to the SNR or RSSI value of the received RREQ message, the receiver may predict future data transmission rate from RREQ transmitter.
- T_{Queue} is the average queuing delay of a data packet at the RREQ receiver. The values of T_{Queue} can be derived analytically using queuing theory under generic assumptions, or can be statistically profiled at each sensor. In BRIT, we adopt the statistical method to calculate the average value of T_{Queue} . In fact, T_{Queue} is approximated by the queue length times T_{MAC} .
- $S_{forward}$ is a vector, which can take either positive or negative values.

Eq. (7) combines several path evaluation criteria into a single metric for path selection purposes. The criteria combines information from several layers, such as the MAC layer latency, DLL layer queuing delay, PHY layer transmission rate, and sensor location information, thereby providing a comprehensive cross-layer perspective to the routing protocol designs.

RREQ Relaying Delay Based on Forwarding Speed:

After computing the “forwarding speed” metric, we use it to calculate the RREQ forwarding delay, which is the amount of time a node holds back the RREQ message. In order to achieve lower packet delivery latencies, the RREQ message forwarding delay is inversely proportional to the forwarding speed of the RREQ receiver. That is, the RREQ messages on sensor with higher forwarding speed will be re-broadcast sooner than the others. The magnitude of the RREQ message replying delays range from tens of milliseconds up to several seconds.

In general, Eq. (7) enables a route selection mechanism to choose faster routing path with higher data rates and lower queuing delays. Accordingly, transmissions along hollow space in the tunnels will be preferred over near-surface transmission along the tunnel walls.

4.2 Route Suppression

On the other hand, as we can see in Fig. 7, the route discovery process is essentially a flooding operation, where every node in the network forwards the RREQ message for at least once. The effect of such flooding operation is similar to “avalanche” phenomena in which the number of RREQ grows quickly so as to guarantee that the route discovery process find at least one path to the destination if it so exists.

However, in underground tunnel environments, such flooding operation is an extremely energy-expensive mechanism, and unnecessary because we usually deploy more than enough sensor nodes in order to provide network reliability.

Hence, we propose an RREQ suppression mechanism in BRIT. As we mentioned earlier in RREQ message relaying operation during the route discovery phase, each node forwards RREQ message after a delay, which was inversely proportional to the the forwarding speed estimated by the RREQ receiver. In order to reduce duplicate transmission of RREQ messages, BRIT further requires that

- 1) Any node forwards the same RREQ message for only once.
- 2) Each RREQ message has a TTL (time-to-live) period that corresponds to a real-time limit, such as 5 seconds. In this case, TTL is not a hop count.
- 3) Any node that overhears an RREQ message and has not already relayed the RREQ message will re-calculate the RREQ forwarding speed based on the newly received RREQ message. This way, on one hand, we guarantee that nodes with better routing metric relay the RREQ message sooner, and on the other, we can expire RREQ messages on nodes with less optimal metrics. In addition, we do not arbitrarily remove RREQ messages altogether on nodes overhearing the RREQ, because there could be extreme scenarios where only these nodes can provide a path to the destination.
- 4) When the TTL of the RREQ message expires, the RREQ message is dropped.

Fig. 8 illustrates how the RREQ suppression mechanism works to further delay some of the sensors to forward the

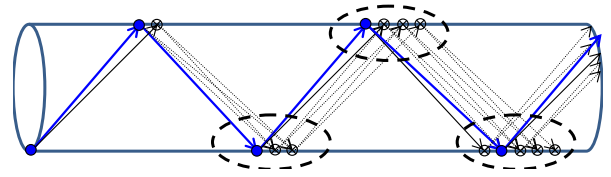


Fig. 8. RREQ Message Suppression in BRIT Routing Protocol.

RREQ messages in the underground tunnel environments. The sensors which may delay their RREQ messages, and eventually cancel their RREQ messages in their relay buffer are indicated by crossed-out circles, and the canceled RREQ transmissions are indicated by dashed lines.

5 Performance Evaluations

5.1 Simulation Setup

We implemented and simulates BRIT along with the 3D underground tunnel model and the signal propagation model using NS2 [17], and compare the performance of BRIT routing protocol with that of AODV in the same simulation scenarios.

The wireless sensor network is created by placing 100 sensor in a 100 m long and 4m wide cylindrical tunnel according to the different deployment strategies that we provided in Section 2, namely, line-up, spiral, random and bipartite deployments. Each sensor is equipped with a UWB transceiver that is capable of transmitting and receiving at a single 20Mbps data rate.

In our experiments, the transmit power is set to 1.4mW, and the threshold of received power is set to 1.4×10^{-11} Watts. The signal propagation model follows our hybrid model as specified in Section 3.

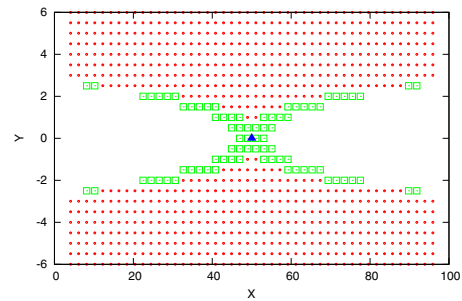


Fig. 9. The Simulated Propagation Model in Underground Tunnels.

Using these parameters and models in the simulations, we calculated the signal reception conditions at various locations of the tunnel inner surface, assuming that one transmitter is placed at the center ceiling of the tunnel, i.e. location (50m, 0m, 2m) in the tunnel. Fig. 9 illustrates the points that got the signals under the free-space and two-ray propagation

models, respectively. In Fig. 9, we could see that the free-space propagation model dominates most part of the tunnel surface areas, and the two-ray propagation only plays a role for the near surface propagation conditions.

Fig. 6 and 9 indicates that the BRIT routing protocol in analogue of a bouncing ball through a tube fully takes advantage of the free-space propagation model in tunnels, and yields the optimal forwarding performance in tunnel environments.

We conducted 10 simulations with different sensor deployments and initial seeds, through which we compute the average values of the performance measurements. In each of the simulations, we created a single CBR traffic stream between a pair of source and destination sensor, and each of the simulations ran for 300 seconds.

5.2 Result Analysis

Fig. 10 compares the network deployment impacts on the network performance in terms of the network throughput, packet loss rates, packet delays and the BRIT routing overhead represented by the number of RREQ/RREP routing control message transmissions.

Fig. 10(a) shows the network throughput differences between AODV and BRIT routing protocols, as well as those of different deployment strategies. Because of the “forwarding speed” metric utilized in BRIT, we could integrate various performance-impacting factors into a single metric, and select the optimal path in the simulations in BRIT. Whereas, AODV’s hop distance metric which does not consider nodal queuing status and link quality information performs worse in all almost all deployment scenarios, except for the line-up strategy. This is due to the fact that the signal propagation model is purely based on two-ray ground model, in which signal strength falls quickly as the distance between the transmitter and receiver increases, as shown in Eq. 2. In such scenarios, AODV would choose less hops than BRIT in line-up sensor deployments because BRIT would choose shorter hop-by-hop distances after comparing the signal quality using Eq. 7. This path selection decision is also reflected in the following Fig. 10 (b), in which the packet loss rate in BRIT is higher than that in AODV. Accordingly, the data delivery delay appears lower in BRIT than that in AODV because many long-latency packets are not delivered at last.

In addition, we could see that the network through stays fair stable in BRIT routing protocol in Fig. 10(a), whereas the network throughput using AODV varies. This is due to the fact that AODV uses RREQ flooding in the initial route discovery phase, which could cause excessive RREQ packet collisions, thus may yield suboptimal paths occasionally.

Fig. 10 (b) shows the packet loss rate for different deployments under BRIT and AODV. It is obvious that the loss rate under BRIT routing is lower than AODV, and that the spiral and random deployments still perform better than other deployments in all the test cases. Especially, the spiral deployments has the least low loss rates among all the deployment strategies. The performance is not changed much for line-up deployment because it does not fully utilize the geographic and structural features, and the three dimensional location in

tunnel to transmit data, which is a basis for our underground tunnel propagation model and BRIT routing protocol.

Fig. 10(c) shows the delays of packets sent at different times of the simulation periods. Except for the line-up deployment strategy, all others perform stable and spiral and random deployments perform best in terms of packet delays.

Fig. 10(d) is an evaluation of the routing control overhead reflected in the number of total RREQ messages sent by source node in each of the ten experiments. BRIT uses much less routing control messages than AODV due to the route suppression mechanisms, and the spiral and random sensor deployment strategies again yield the best performance with the least number of RREQ messages. The total number of RREQ messages for establishing the path between a single source and destination pair is around 6 in spiral and random deployment strategies for BRIT.

From above simulation results and analysis, we could see that the spiral deployment is the most preferable strategy in tunnel wireless sensor networking environments, because it more effectively creates free-space propagation chances between successive sensor on the forwarding paths. The performance of the random deployment comes the second, but is not as stable as that of the spiral deployment in various experiment cases.

In addition, we conclude that routing based on BRIT is more suitable for underground tunnel routing scenarios than other traditional routing protocols, such as AODV. In terms of deployment strategies, we recommend the spiral deployment due to its stable and higher quality service than other deployment strategies in underground tunnel environments.

6 Conclusions

Our research is a first step towards modeling underground tunnels and designing underground tunnel routing protocols in a holistic manner. Specifically, we proposed a routing protocol, called BRIT, under the studied signal propagation and deployment models for data communication purposes in underground tunnel environments. The performance of BRIT is evaluated using simulations and compared against that of AODV as a bottomline, which proves the obvious advantage of the cross-layer design perspectives in BRIT. The contributions of our research presented in this paper are the following:

- Wireless sensor networks are not to be treated as a generic platform that is designed once for all, but a living organism that have to be customized in a holistic manner in order to meet the stringent requirements for efficiency.
- The factors to be considered in designing multi-hop wireless sensor network include deployment patterns, signal propagation, traffic characteristics. According to our simulations, the spiral deployment appeared optimal for wireless sensor network in the underground tunnel environments.
- We defined a forwarding speed metric for route selections. It is a meaningful metric that integrates location, distance, signal quality, data rate, traffic queuing situation all together, and is a comprehensive and unified metric for cross-layer designs.

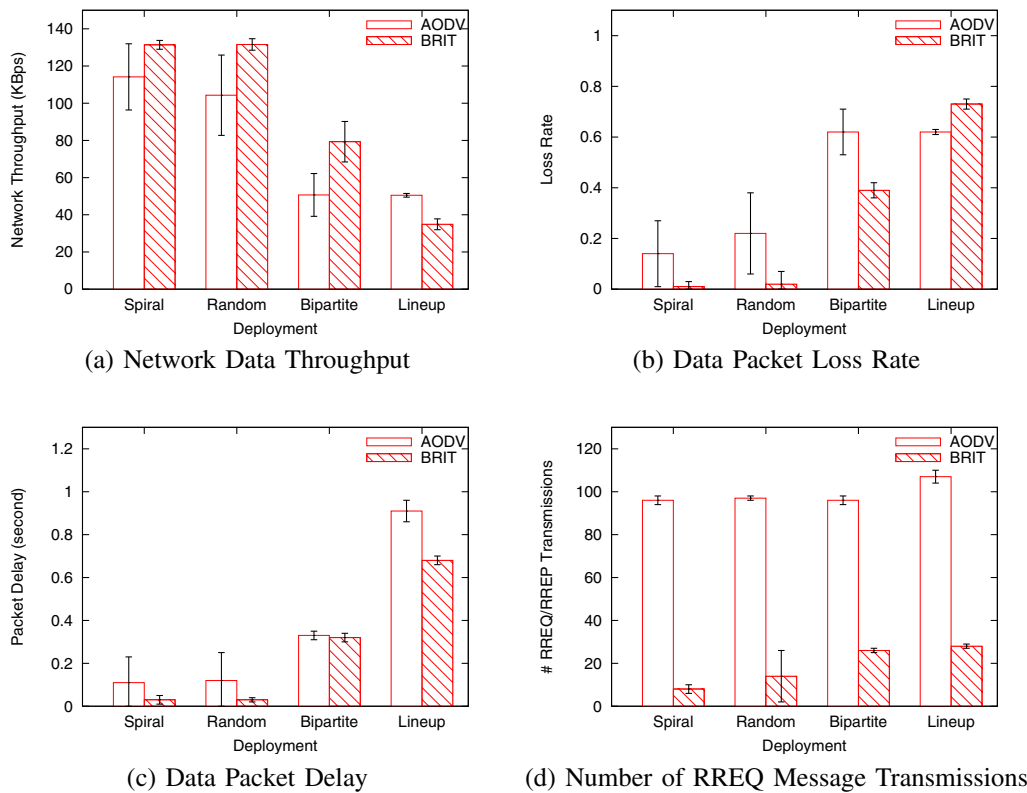


Fig. 10. Performance Comparisons of AODV and BRIT in Different Sensor Network Deployments.

References

- [1] S. M. Nazrul Alam and Zygmunt J. Haas. Coverage and Connectivity in Three-Dimensional Networks. In *Proceedings of the 12th annual international conference on Mobile computing and networking*, pages 346–357. Los Angeles, CA, USA, 2006.
- [2] N. Arad and Y. Shavitt. Minimizing Recovery State in Geographic Ad-Hoc Routing. In *Proceedings of the 7th ACM international symposium on Mobile ad hoc networking and computing*, pages 13–24. Florence, Italy, 2006.
- [3] A. Basu, J. Gao, J.S.B. Mitchell, and G. Sabhnani. Distributed localization using noisy distance and angle information. In *Proceedings of the 7th ACM international symposium on Mobile ad hoc networking and computing*, pages 262–273. Florence, Italy, 2006.
- [4] M.-G. Di Benedetto and G. Gianloca. *Understanding Ultra Wideband Radio Fundamentals*. Prentice Hall, Upper Saddle River, NJ, 2004.
- [5] J. Bruck, J. Gao, and A. Jiang. Localization and routing in sensor networks by local angle information. In *Proceedings of the 6th ACM international symposium on Mobile ad hoc networking and computing*, pages 181–192. Urbana-Champaign, IL, USA, 2005.
- [6] A.G. Emslie and R. L. Theory of the Propagation of UHF Radio Waves in Coal Mine Tunnels. *IEEE Transactions on Antenna And Propagation*, 23(2):192–205, 1975.
- [7] Sheng H., P. Orlik, A.M. Haimovich, L.J. Cimini Jr., and Zhang J. On the spectral and power requirements for ultra-wideband transmission. In *IEEE International Conference on Communications*, pages 738–742. Anchorage, A K, USA, 2003.
- [8] D.B. Johnson, D.A. Maltz, and Y.C. Hu. The Dynamic Source Routing Protocol for Mobile Ad Hoc Networks (DSR). Technical report, IETF MANET Working Group, Jul. 2004.
- [9] T.S. Kim, H. Lim, and J.C. Hou. Improving Spatial Reuse Through Tuning Transmit Power, Carrier Sense Threshold, and Data Rate in Multihop Wireless Networks. In *Proceedings of the 12th annual international conference on Mobile computing and networking*, pages 366–377. Los Angeles, CA, USA, 2006.
- [10] S. Lee, B. Bhattacharjee, and S. Banerjee. Efficient geographic routing in multihop wireless networks. In *Proceedings of the 6th ACM international symposium on Mobile ad hoc networking and computing*, pages 230–241. Urbana-Champaign, IL, USA, 2005.
- [11] F. Li, P. Han, X. Wu, and W. Xu. Research of UWB Signal Propagation Attenuation Model in Coal Mine. *Ubiquitous Intelligence and Computing*, 4611(2007):819–828, August 2007.
- [12] M. Li and Y. Liu. Rendered Path: Range-Free Localization in Anisotropic Sensor Networks with Holes. In *Proceedings of the 13th annual international conference on Mobile computing and networking*, pages 51–62. Montreal, Quebec, Canada, 2007.
- [13] M. Li and Y. Liu. Underground structure monitoring with wireless sensor networks. In *Proceedings of the 6th international conference on Information processing in sensor networks*, pages 69–78. Cambridge, Massachusetts, USA, 2007.
- [14] T. Melodia, M. C. Vuran, and D. Pompili. The state-of-the-art in cross-layer design for wireless sensor networks. *Springer Lecture Notes in Computer Science (LNCS)*, 2006.
- [15] C. Nerguizian, C.L. Despins, S.A., and M. Djadel. Radio Channel Characterization of an Underground Mine at 2.4Ghz. *IEEE Transactions on Wireless Communication*, 4(5):2441–2453, September 2005.
- [16] C. Perkins, E. Belding-Royer, and S. Das. RFC 3561 - Ad hoc On-Demand Distance Vector (AODV) Routing. Technical report, Internet Engineering Task Force (IETF), Jul. 2003.
- [17] VINT Project. The Network Simulator - ns-2. <http://www.isi.edu/nsnam/ns/>.
- [18] T.S. Rappaport. *Wireless Communications Principles and Practice*. Prentice Hall, Upper Saddle River, NJ, 1996.
- [19] Yue Wang, Jie Gao, and Joseph S.B. Mitchell. Boundary Recognition in Sensor Networks by Topological Methods. In *Proceedings of the 12th annual international conference on Mobile computing and networking*, pages 122–133. Los Angeles, CA, USA, 2006.
- [20] T. B. Welch, M.J.Walker, and R.A.Foran. Very Near Ground RF Propagation Measurements and Analysis. *Wireless Personal Communications*, 536(2000):1–9, April 2006.
- [21] M.Z. Win and R.A. Scholtz. Ultra-wide bandwidth time-hopping spread-spectrum impulse radio for wireless multiple-access communication. *IEEE Transaction on Communication*, 48(4):679–671, 2000.